Lab on a Chip

Dynamic Article Links

Cite this: *Lab Chip*, 2012, **12**, 923

www.rsc.org/loc

PAPER

Locally enhanced concentration and detection of oligonucleotides in a plug-based microfluidic device

Wei-Feng Fang, Shang-Chieh Ting, Ching-Wen Hsu, Yu-Tzu Chen and Jing-Tang Yang*

Received 23rd September 2011, Accepted 16th December 2011
DOI: 10.1039/c2lc20917a

We propose a novel technique that allows oligonucleotides with specific end-modification within a plug in a plug-based microfluidic device to undergo a locally enhanced concentration at the rear of the plug as the plug moves downstream. DNA was enriched and detected *in situ* upon exploiting a combined effect underlain by an entropic force induced through fluid shear (*i.e.* a hydrodynamic-repellent effect) and the interfacial adsorption (aqueous/oil interface) attributed to affinity. Flow fields within a plug were visualized quantitatively using micro-particle image velocimetry (micro-PIV); the distribution of the fluid shear strain rate explains how the hydrodynamic-repellent effect engenders a dumbbell-like region with an increased concentration of DNA. The concentration of FAM (6-carboxy-fluorescein)-labeled DNA (FC-DNA) and of TAMRA (tetramethyl-6-carboxyrhodamine)-labeled DNA (TC-DNA), respectively, and the hybridization of probe DNA (modified with FAM) with target DNA (modified with TAMRA) were investigated in devices; a confocal fluorescence microscope (CFM) was utilized to monitor the processes and to resolve the corresponding 2D patterns and 3D reconstruction of the DNA distribution in a plug. TC-DNA, but not FC-DNA, concentrating within a plug was affected by the combined effect so as to achieve a concentration factor (C_r) twice that of FC-DNA because of the lipophilicity of TAMRA. Using fluorescence resonance-energy transfer (FRET), we characterized the hybridization of the DNA in a plug; the detection limit of a system, improved by virtue of the proposed technique (the locally enhanced concentration), for DNA detection was estimated to be 20–50 nM. This technique enables DNA to concentrate locally in a nL–pL free-solution plug, the locally enhanced concentration to profit the hybridization efficiency and the detection of DNA, prospectively serving as a versatile means to accomplish a rapid DNA detection in a small volume for a Lab-on-a-Chip (LOC) system.

Introduction

The exploitation of plugs or droplets in microchannels has emerged as a powerful technique that attracts much attention and is widely applied for the synthesis of advanced materials,[1] biological assay,[2,3] drug discovery[4] and biochemical kinetics,[5] attributed to the key characteristics of compartmentalization, high-throughput handling and great versatility. The rapid mixing and reaction of fluids are readily achieved using plug- or droplet-based microfluidics.[6] The formation frequency, volume, composition, concentration, moving speed/period and the surrounding condition of a plug in a microchannel are all readily controllable with the modulation of flow rates of the carrier fluids (immiscible fluids) and sample fluids (aqueous fluids) to facilitate investigations of biochemical reactions occurring in plug-based microfluidic systems.

Department of Mechanical Engineering, National Taiwan University, Taipei, 10617, Taiwan. E-mail: jtyang@ntu.edu.tw; Fax: +886-(2)-2363-4254; Tel: +886-(2)-3366-9875

A plug-based microfluidic technique enabled monitoring of the crystallization of proteins in a plug; those crystals were analyzed with X-ray diffraction.[7] Expression of proteins *in vitro* within a droplet was also exhibited with this technique.[8] The clotting duration of blood was estimated in a plug-based device with an activated partial thromboplastin time (APTT) test.[9] A rapid detection of bacterial susceptibility to antibiotics without pre-incubation[10] and the growth and proliferation of cells within droplets for several days[11] were achieved using plug-based microfluidics. A digital microfluidic chip was developed effectively to perform real-time polymerase chain reaction (RT-PCR) amplification within a picolitre droplet.[12] An enrichment based on microdroplet PCR was proposed for parallel amplifications of specific subsets of the human genome for targeted sequencing.[13] Streptavidin-biotin-based fluorescence resonance-energy transfer (FRET) was utilized to realize a droplet-based DNA assay.[14] A technique involving FRET with a molecular beacon (MB) as a sensing probe was proposed for label-free DNA detection in a plug-based system in seconds.[15]

This journal is © The Royal Society of Chemistry 2012

As outlined above, numerous authors have so far focused on biochemical reactions or assay in a plug, but the concentration or purification of biomolecules in a plug remains a significant and pending issue. In continuous-flow microfluidics, the concentration or purification of samples—a crucial unit operation—would be accomplished by virtue of continuous-flow separation methods.[16] With regard to the concentration or enrichment of DNA in microfluidic systems, a microchip-based capillary electrophoresis (CE) system,[17] solid-phase extraction (SPE)[18] and electrophoretic separation in gels and nanostructures[19] are efficient techniques to separate a specific nucleic acid (DNA) selectively from other biological entities in a medium solution. The microfabricated capillary array electrophoresis (μCAE) system with 96 microchannels, fabricated on a glass wafer (diameter 150 mm), was exploited to perform DNA sequencing with a large throughput; this system offered an effective separation length 15.9 cm of DNA fragments and thereby produced sequencing data at a rate of 1.7 kbp min^{-1}.[20] Microchip electrophoresis (ME) with programmed field strength gradients (PFSG) was proposed to decrease the duration of analysis, which was one fifteenth that for conventional ME, during the separation of a 100 bp DNA ladder.[21] The purification of DNA from a biological sample in the form of whole blood was demonstrated in a glass microchip, in which silica beads were immobilized with sol–gel in a channel to provide a solid phase onto which DNA was adsorbed.[22] A microfluidic particle-separation device with an obstacle matrix was reported to separate bacterial artificial chromosomes in 10 min with a resolution of approximately 12% using an asymmetric bifurcation effect of laminar flow around obstacles.[23] Genomic DNA (gDNA) was purified from whole cell lysates in a photo-activated polycarbonate (PPC) microfluidic chip with a bed consisting of an ordered micropost-array.[24] Size-based and charge-based separation of DNA and proteins was realized in a device with an anisotropic sieving structure composed of a two-dimensional nano-structural array.[25] A PDMS microchannel possessing a three-dimensionally sculptured nano- or micro-composite structure was utilized to separate DNA mixtures with distinct base pairs.[26] A laser-irradiated magnetic-bead system (LIMBS) was designed to lyse bacterial cells, to extract and to detect the corresponding DNA by combining laser irradiation lysing and magnetic bead-based separation.[27] Concentration enrichment of DNA in a microfluidic device, in which a hydrogel microplug[28] or a polyacrylamide gel bank[29] was fabricated, was accomplished using gel electrophoresis based on electrokinetics. The use of an electric-field isolator (EFI) was an alternative technique that enabled isolation of DNA inside a selected location, thus concentrating the DNA.[30]

These approaches require micro- or nano-structures, a porous medium, gels, highly viscous polymer solutions, microbeads or magnetic beads to concentrate or to purify DNA within a biological sample in a microchannel, indicating that concentration or purification of DNA is quite difficult in free solution.[19] Despite these approaches being effective, underlying drawbacks exist such as the complicated fabrication required for an entire device or platform, a large loss of pressure caused by solid obstacles or filled materials, a burdensome procedure and external fields (electric or magnetic field) involved in a continuous separation. Moreover, the investigation of the concentration of species in a plug is scarce but indispensable for plug-based microfluidics, especially for the concentration or enrichment of oligonucleotides.

Here we suggest a novel technique for oligonucleotides with specific end-modification to be locally concentrated within a plug (free solution state) in a plug-based microfluidic device based on a combined effect involving hydrodynamic repulsion and affinity adsorption. A concentration of oligonucleotides was realized within a micro-plug with a volume from nL to pL in seconds. We demonstrated that this technique enabled highly efficient hybridization of DNA and its detection at a concentration of ~20 nM in terms of the concept of locally enhanced concentration.

Notion of a localized concentration of DNA

The proposed technique to enhance locally the concentration of DNA within a plug is illustrated in Fig. 1. Fig. 1(a) left shows a simple flow focusing device (FFD) of width 100 μm, depth 103 μm, and length 28 mm designed to generate a plug of length approximately 400 μm (volume ≈ 4 nL). In general, the distribution of molecules within a plug would be uniform or accumulated at the end regions near an aqueous/oil interface as the plug is generated upstream. In the case of an accumulation, the interfacial adsorption activity for proteins in a plug was characterized using specifically oil-soluble surfactants that adsorbed proteins at the aqueous/oil interface.[31] Here we suggest a method for DNA in an aqueous plug adsorbed at an aqueous/oil interface based on an affinity effect as shown in Fig. 1 right. For instance, DNA labeled with FAM (6-carboxy-fluorescein) is not adsorbed on an oily liquid that is uniformly distributed within a plug, whereas a specifically end-modified molecule of DNA labeled with TAMRA (tetramethyl-6-carboxyrhodamine) possesses a chemical polarity analogous to that of oil molecules, enhancing its susceptibility to gather and to become adsorbed near the aqueous/oil interface. According to this affinity effect, DNA with a specific modification would concentrate near an aqueous/oil interface.

Apart from that affinity effect, the flow fields within a liquid plug are capable of impacting the distribution of DNA, which is deemed a hydrodynamic effect that is partially responsible for the localized concentration of DNA. Two recirculating flows that exist primarily within a liquid slug of a liquid–liquid slug flow[32–34] are generally a pair of counter-rotating vortices with a structurally elongated shape. From the perspective of hydrodynamics, regions occupied by recirculating flows are likely to be subject to a large shear strain rate that is indicative of the strength of the shear stress of the fluid.

In this work, we utilized micro-particle image velocimetry (micro-PIV) to visualize quantitatively the internal flow fields of an aqueous plug produced in our plug-based microfluidic device; the recirculating flows were also observed, as schematically illustrated in Fig. 1(b) left. Specific regions were laden with DNA molecules in an aqueous plug; those regions were evidently subject to small shear strain rates. Alternatively stated, it is difficult for DNA molecules to enter regions with large shear strain rates that seem to act to repel the DNA molecules. Moreover, the conformation of regions laden with DNA molecules jointly resembles a dumbbell, which is an anomalous phenomenon that seems not to have been reported in the

 This journal is © The Royal Society of Chemistry 2012

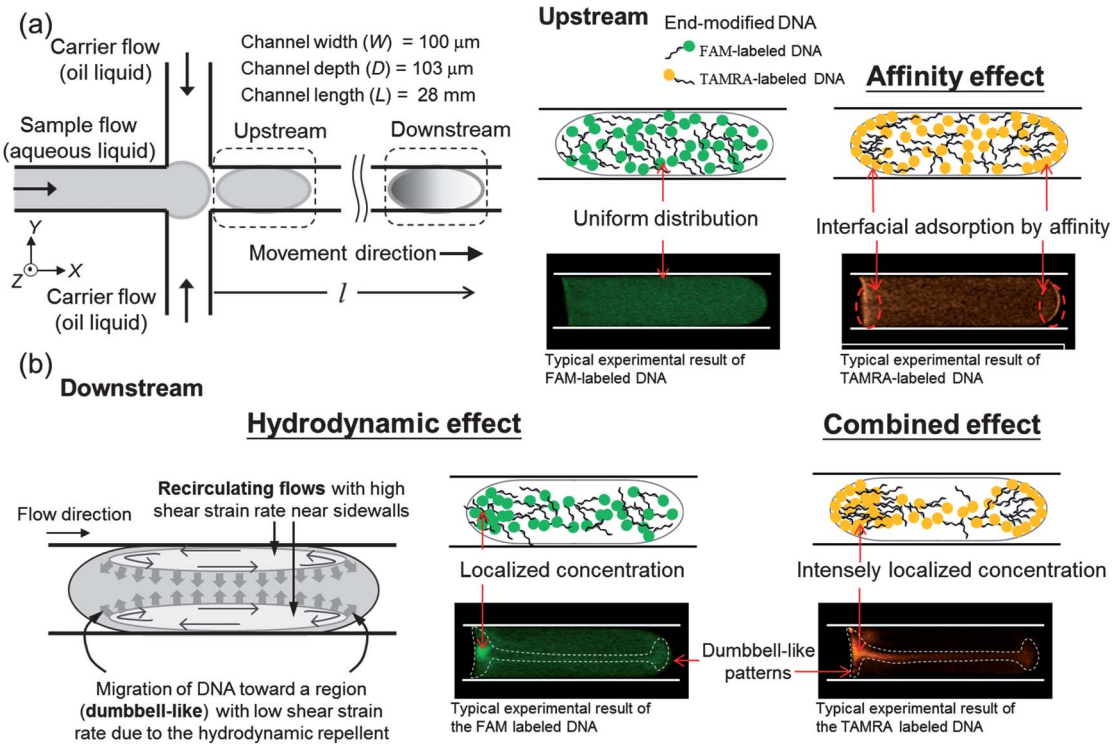

Fig. 1 Schematic diagram of a locally enhanced concentration of DNA in a plug. (a) Illustration of a simple flow-focusing device, FFD to generate a plug (left) and a concept diagram of the affinity effect (right); *l* is the downstream distance. (b) Concept diagrams of the hydrodynamic effect (left) and the combined effect (right). The denoted flowing directions are with respect to a frame of reference moving with the plug. The gray thick arrows signify the direction of DNA migration. The region enclosed with a dashed white curve presents a dumbbell-like shape.

literature on plug-based microfluidics. As DNA molecules gather locally in such a dumbbell-like region through that hydrodynamic effect, their concentration is also enhanced.

To augment the localized concentration of DNA in a plug, we initiated a novel technique, taking advantage of a combination of the affinity effect and the hydrodynamic effect as shown in Fig. 1(b) right. As a plug with TAMRA-labeled DNA moves downstream, the affinity effect reinforces the DNA, repelled from the sidewalls by the hydrodynamic effect, to migrate to a region of small shear strain (a dumbbell-like region), and to accumulate there. Most DNA gathered near the rear of the plug, forming a locally enhanced concentration, which we discuss in a subsequent section.

Materials and methods

Microfabrication

The plug-based microfluidic device was fabricated according to a soft lithographic procedure of poly(dimethylsiloxane) (PDMS) involving a fabrication of a mold and a PDMA replication.[35] A negative photoresist (SU-8 2035, MicroChem Corp.) was fabricated on a silicon wafer, to serve as a master mold, based on a standard photolithographic technique including wafer cleaning, photoresist spinning, soft baking, UV exposure, post-exposure baking, developing and hard baking. PDMS solution, a mixture 10 : 1 (by mass) of silicon elastomer (Sylgard 184) and curing agent (Dow Corning Corp.), was in sequence degassed, poured into the master mold and cured on a hot plate at 80 °C for 2 h. The cured PDMS (PDMS replica) was then peeled from the mold; holes were drilled at the inlet and outlet locations on the PDMS. After the surface of the PDMS replica and a cover slide were treated with oxygen plasma, the device was obtained upon bonding the replica and the slide. The device was finally baked in an oven at 100 °C over 24 h to ensure that the surface of the channel restored its hydrophobicity.

Experimental setup and sample solutions

We employed micro-particle image velocimetry (micro-PIV) with an epi-fluorescence microscope to resolve the flow field in a plug so as to interpret the enrichment of DNA. The seeding particles added to the aqueous plug were fluorescent polystyrene particles (diameter 500 nm, density 1.05 g cm^{-3}) (Duke Scientific, $\lambda_{ex}/\lambda_{em}$ = 542/612 nm). To record the particle track in the plug we used an inverted fluorescent microscope (Nikon Eclipse Ti-U, Japan) that possessed an objective lens with amplification 60× (Plan Apochromat VC60×, numerical aperture 1.2) and a high-speed camera (Phantom v310, Vision Research, USA, frame rate 2000 fps). The field of view (FOV) was about 250 × 250 μm (512 × 512 pixels) corresponding to a spatial resolution 0.488 μm per pixel. The captured images were processed with a standard cross-correlation scheme (Insight 3G, TSI Inc.) applying an interrogation window of size 32 × 32 pixels to calculate the velocity field.

We utilized a confocal fluorescence microscope (CFM) to record and to analyze experiments encompassing a concentration test, a mixing test and a reaction test. The confocal microscope system (Nikon A1R, Japan) adopted a resonant scanning head to

capture rapidly an image with a temporal resolution of 230 fps, and an objective lens with 10 times amplification (Plan Apochromat 10×, numerical aperture = 0.45) to obtain an image with lateral resolution (*XY* plane) 512 × 64. A pinhole used to eliminate light outside the focal plane was set at 1.5 μm, near 1 Airy unit (AU) of the system. The axial resolution of the system was approximately 5 μm.

Silicone oil (100% poly(dimethylsiloxane), SIL-5000® Silicone Oil, Dutch Ophthalmic, USA) that was adopted as a carrier flow possessed a kinetic viscosity of 100 $mm^2 s^{-1}$, a density of 97 $kg m^{-3}$ and a surface tension of 20.9 $mN m^{-1}$ at 25 °C. Fluorophore-labeled DNA oligonucleotides (powder, MDBio Inc., Taiwan) were dissolved in a phosphate-buffered saline solution (DPBS, Thermo Scientific HyClone) at pH 7.4; the concentration of these sample solutions was 5 μM. We chose 10-mer oligonucleotides (diffusion coefficient ≈ 10^{-10} $m^2 s^{-1}$), which were labeled with FAM (6-carboxy-fluorescein, $\lambda_{ex}/\lambda_{em}$ = 495/521 nm) and TAMRA (tetramethyl-6-carboxyrhodamine; $\lambda_{ex}/\lambda_{em}$ = 560/583 nm) respectively to perform the experiments; FAM possesses a hydrophilic functional group whereas TAMRA possesses a lipophilic one.

The relevant information of DNA for the tests is listed in Table 1. For the concentration test, several dozens of FAM-labeled DNA and TAMRA-labeled DNA with diverse sequences were tested, revealing that the concentration was independent of the DNA sequence. We therefore exhibit and discuss typical results pertaining to the concentration of FC-DNA (5′-FAM-CCTAGCCCCT-3′) and of TC-DNA (5′-TAMRA-CCTAGCCCCT-3′) in a plug respectively in a subsequent section. Fluids A and B represent fluids injected into a plug-based microfluidic device; Fluid A is a probe DNA (5′-FAM-CAGGTCAGGT-3′) solution and Fluid B is a PBS buffer solution for the mixing test whereas Fluid A is a probe DNA (5′-FAM-CAGGTCAGGT-3′) solution and Fluid B is a target DNA (5′-TAMRA-ACCTGACCTG-3′) solution for the reaction test. The melting temperature of the probe DNA and the target DNA is 32 °C. All tests were executed at 25 °C and 50% humidity. Sample solutions were injected into each inlet of the device with a syringe pump (230 series, Kd Scientific Inc.); the volumetric flow rate operated at 0.1–2.0 μL min^{-1}. The capillary number (Ca) for the plug operation in the test was from 1 × 10^{-3} to 1.2 × 10^{-2}.

In the concentration test, light (488 nm, Ar-ion laser) excited FC-DNA, and the resulting emission was filtered with a band-pass filter (500–550 nm); the filtered light was detected with a photomultiplier tube (PMT). Light (561 nm, solid-state laser) excited TC-DNA, and the resulting emission was filtered with a band-pass filter (570–600 nm); the filtered light was detected by the PMT. In the mixing test, the probe DNA was excited at 488 nm and the filtered emission was detected with the PMT. For the reaction test, by means of fluorescence resonance-energy transfer (FRET),[36] we monitored the hybridization of the probe DNA and the target DNA within a plug in the device. FRET involves energy transfer such that an excited donor molecule (such as FAM) emits light that excites an acceptor molecule (*e.g.* TAMRA) if these molecules are conjugated or sufficiently close (<~10 nm); FAM and TAMRA constitute a common FRET pair. Light (488 nm) excited the DNA and the corresponding emissions of FAM and TAMRA were simultaneously detected with a separate PMT. A detailed illustration of this approach was reported in our previous work.[37] The image processing and acquisition were achieved with commercial software (NIS-Elements AR, Nikon, Japan).

Table 1 Properties of DNA solutions for the tests; the concentration of all solutions is 5 μM

Test	Name	Sequence
Concentration test	FC-DNA	5′-FAM-CCTAGCCCCT-3′
	TC-DNA	5′-TAMRA-CCTAGCCCCT-3′
Mixing test	Probe DNA (Fluid A)	5′-FAM-CAGGTCAGGT-3′
	PBS (Fluid B)	—
Reaction test	Probe DNA (Fluid A)	5′-FAM-CAGGTCAGGT-3′
	Target DNA (Fluid B)	5′-TAMRA-ACCTGACCTG-3′ (complementary to probe DNA)

Results and discussion

Analysis of the flow field and rate of shear strain in a plug

In Fig. 2, we show representative results of measurement of the internal flow fields in the front and rear parts of an aqueous plug, which are structurally consistent with that depicted in Fig. 1(b). The color contours signify the magnitude of the shear strain rate of the fluid, theoretically defined as

$$\sigma_{xy} = \frac{1}{2}\left(\frac{\partial v}{\partial x} + \frac{\partial u}{\partial y}\right) \quad (1)$$

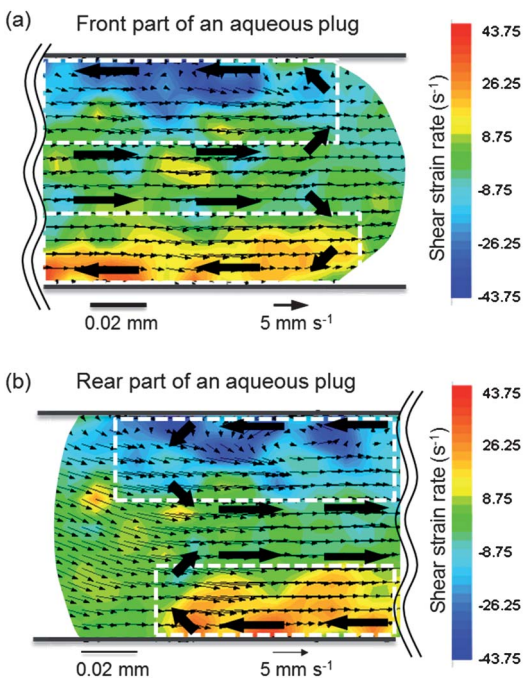

Fig. 2 Representative measurements of internal flow fields in the front (a) and rear (b) parts of an aqueous plug. The velocity vectors shown here are with respect to a frame of reference moving (from left to right) within the plug. The color-coded contours represent the magnitude of the shear strain rate. Regions subject to a large shear strain rate are particularly highlighted with dashed white rectangles. The thick black arrows signify the flowing directions.

This journal is © The Royal Society of Chemistry 2012

in which u and v are respectively the fluid velocity components in directions x and y of a two-dimensional Cartesian coordinate system. The shear stress of the fluid is proportional to the shear strain rate: the fluid viscosity is the factor of proportionality. Two elongated recirculating regions are clearly recognizable within the plug, which are adjacent to the upper and lower sidewalls of the microchannel; these regions are subject to large shear strain rates. As already mentioned (in the section Notion of a localized concentration of DNA), the concentration of DNA was much smaller in the recirculating regions than elsewhere, implying that recirculating regions (inherently subject to large shear strain rates) had a repellent effect upon DNA molecules. This anomalous phenomenon is speculated to arise from an entropic force corresponding to a principle of maximum entropy production (MEPP) that dictates the direction of evolution of natural processes, according to the second law of thermodynamics.[38] Consistent with MEPP, an evolving non-equilibrium dissipative system intrinsically tends to maximize its entropy production, which is phenomenally and statistically imagined as the result of an action of an entropic force in the system.

The dynamic behavior of DNA is reported also to be affected substantially by this entropic force.[39,40] DNA molecules are biopolymers of a kind with evident structural flexibility, which undergo conformational changes driven by an entropic force.[41,42] When placed in a shear flow, a DNA molecule generically exhibits a stretching deformation.[39,43,44] In theory, the stretched state of a DNA molecule has considerably less entropy than the unstretched state (*i.e.* a randomly coiled state).[39,41,42] The entropy of a DNA molecule is conceptually proportional to the extent of the conformational state that a DNA molecule can assume. It is intuitively comprehensible that unstretched DNA tends to have a randomly coiled conformation, which corresponds to greater entropy. In contrast, the conformation of a stretched DNA molecule has a predictability greater than that of an unstretched DNA because a stretched DNA molecule generally has a more straightened configuration. In brief, a stretched DNA has notably less entropy than an unstretched DNA, and thereby has a tendency to resume an unstretched state, so as to maximize the entropy of the system in which it is a part.

Based on the entropic effect described above, one can reasonably infer that, in an aqueous plug, DNA molecules initially situated in regions subject to a large shear strain rate tend to migrate to regions subject to a smaller shear strain rate. This inference conforms to our experimental observation (see the next section) that the DNA concentration was considerably smaller in the recirculating regions than elsewhere. The locally enhanced concentration of DNA in the dumbbell-like region within an aqueous plug is accordingly deemed to result from the action of an entropic force induced by fluid shear stress. Moreover, this entropic force might also account for a peculiar phenomenon that the maximum of DNA concentration at the rear is greater than that at the front. The distribution of the recirculating regions subject to a large shear strain rate is spatially uneven; the regions free of large shear strain rates are dimensionally larger at the rear than at the front (see Fig. 2). Alternatively stated, a greater space to accommodate migrating DNA molecules at the rear than at the front produces a larger maximum of DNA concentration at the rear.

Concentration test

In this test, we analyzed 2D distribution patterns of DNA located at the middle of a plug at varied downstream positions, and a 3D distribution of DNA within a plug at a downstream position of 25 μm as shown in Fig. 3. Fig. 3(a) and (b) respectively show the concentration of FC-DNA and of TC-DNA in a plug with a velocity of 1.8 mm s^{-1} whereas Fig. 3(c) and (d) respectively show the concentration of FC-DNA and of TC-DNA in a plug with a velocity of 3.8 mm s^{-1}. From a comparison of the 2D patterns, the DNA in a plug gradually accumulated at the rear of the plug as the plug moved downstream, demonstrating that the recirculating flows existing in the plug are capable of repelling hydrodynamically the DNA to gather into the dumbbell-like region. Moreover, the plug containing TC-DNA exhibited a strong signal at the oil/aqueous interface, which indicates that part of the TC-DNA adsorbed at the interface through the affinity effect. As the plug moved downstream, owing to the combined effects of hydrodynamics and affinity adsorption, TC-DNA greatly concentrated at the rear of the plug, superior to FC-DNA. As the distribution of DNA within a plug is three-dimensional, a 3D reconstruction image of a plug is essential to estimate quantitatively the degree of DNA accumulating at the rear of the plug. We utilized CFM to reconstruct the 3D distribution of DNA within a plug. It is difficult to obtain instantaneously a 3D distribution of DNA within a plug because of its movement, but the DNA distribution within a plug at a location of a channel is constant over time. We were hence able to scan 2D distribution patterns at various Z-sections at this location using CFM, and then reconstruct a 3D distribution of DNA by stacking the 2D patterns. The Z-interval of two 2D pattern images was set to 5 μm similar to the thickness of the optical slice; twenty 2D pattern images were stacked along the Z-direction in sequence to form a 3D distribution image. This 3D distribution of DNA in a plug is shown in Fig. 2, right row. FC-DNA concentrated at the rear of the plug, which was more remarkable at a plug velocity of 3.8 mm s^{-1} than at 1.8 mm s^{-1}. For TC-DNA, the accumulation zone at a plug velocity of 1.8 mm s^{-1} was larger than at 3.8 mm s^{-1}, but the signal intensity within the zone at the plug velocity of 3.8 mm s^{-1} was larger than at 1.8 mm s^{-1}, indicating that the outcome of the concentration (or accumulative effect) at the plug velocity of 3.8 mm s^{-1} was superior to that at 1.8 mm s^{-1}.

To quantify the degree of the localized concentration or enrichment of DNA at the rear of a plug, a concentration factor (C_f) is defined as $C_f = \bar{I}_{localized}/\bar{I}$, in which $\bar{I}_{localized}$ signifies the mean value of the localized fluorescent intensity of DNA within a volume of interest (VOI, a cube of length 20 μm, located at a zone at which maximum intensity occurs) at the rear of a plug as shown in Fig. 4(a); $\bar{I}$ is the average concentration of a plug. Calibration lines of DNA concentration *versus* fluorescence intensity were established based on previous work;[37] values of R^2 of lines were 0.996 for FAM-labeled DNA and 0.955 for TAMRA-labeled DNA in a display of perfect linearity in a regression analysis (not shown here). It is reasonable to derive the concentration from the intensity according to this calibration.

Fig. 4(b) shows the concentration factors of DNA within the VOI in plugs at various velocities (0.4–5.4 mm s^{-1}); all plugs were

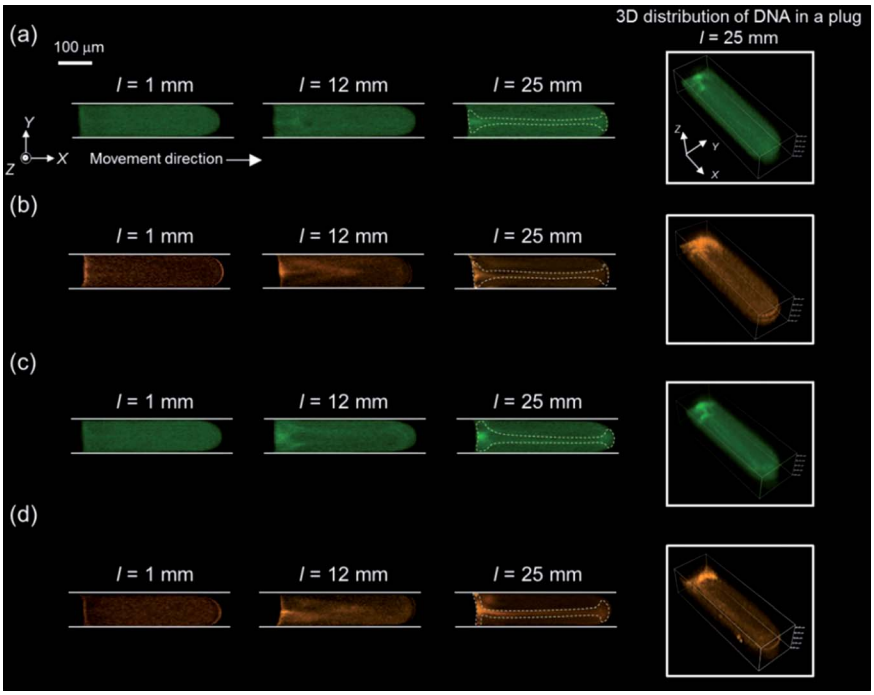

Fig. 3 Two-dimensional distribution patterns and three-dimensional reconstruction of DNA in a plug. Concentration of FC-DNA (a) and TC-DNA (b) at a plug velocity of 1.8 mm s^{-1}, and of FC-DNA (c) and TC-DNA (d) at a plug velocity of 3.8 mm s^{-1}. (The regions enclosed with dashed white lines contain a greater concentration.)

analyzed at a downstream location of 25 mm. The concentration of DNA in a plug was enhanced with increasing plug velocity, consistent with the fact that stronger recirculating flows existed such that more DNA was repelled to accumulate at the rear of the plug. At a plug velocity of 0.4 mm s^{-1}, C_f for FC-DNA was about unity, expressing a feeble accumulation of FC-DNA occurring at the rear of the plug; that is, the internal vortices of the plug were too weak to condense the DNA at the rear. For TC-DNA, the C_f was about 1.65, larger than that for FC-DNA because of the affinity effect on the localized concentration of TC-DNA near an interface. As the plug velocity increased, C_f for FC-DNA approached 2 whereas C_f for TC-DNA approached 4, and also the difference of C_f for FC-DNA and for TC-DNA increased. As the rate of fluidic shear strain increased with increasing velocity of the moving plug, the larger the velocity that the plug possesses, the stronger the hydrodynamic-repellent effect that the recirculating flows induces, which accounts for the increased C_f with increasing plug velocity. The combined effect involving the affinity adsorption and hydrodynamic repulsion played a significant role in concentrating TC-DNA, especially in the case of a large plug velocity. Only 4.6 s was required for FC-DNA to concentrate in a plug, attaining $C_f = 4.0$ at the plug velocity of 5.4 mm s^{-1}.

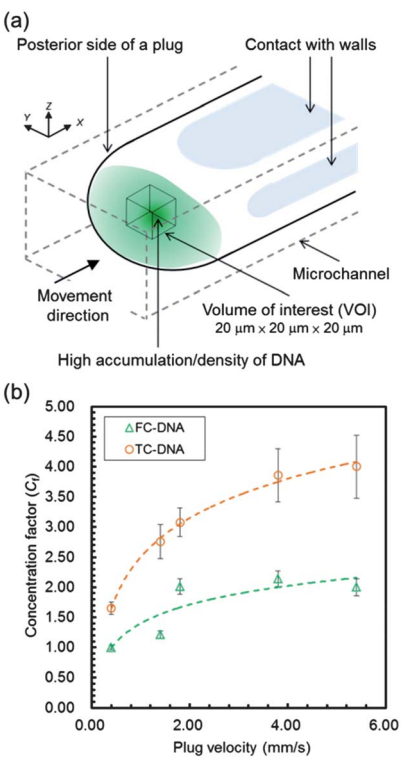

Fig. 4 Quantitative analysis of DNA concentration within a volume of interest (VOI). (a) Schematic diagram of a sampling VOI. (b) Correlation of the concentration factor (C_r) and plug velocity for a DNA concentration.

Mixing and reaction (hybridization) tests

To conduct the mixing and the reaction tests, we designed a plug-based microfluidic device composed of a winding channel with 45 curved units for fluid mixing and reaction, and a straight channel for DNA concentration as shown in Fig. 5(a); sample fluids, A and B, for the tests are listed in Table 1. In the tests, the plug

This journal is © The Royal Society of Chemistry 2012

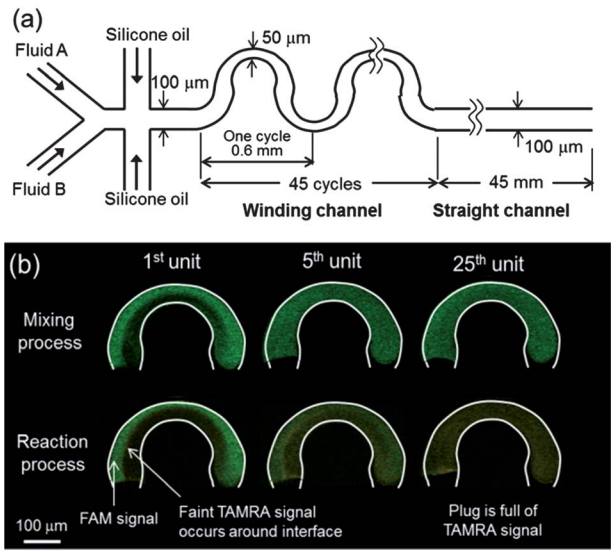

Fig. 5 Mixing and reaction (hybridization) tests in a winding channel. (a) Illustration of a plug-based microfluidic device for DNA mixing, hybridization and concentration. (b) 2D confocal images at various curved units for mixing (upper), and for reaction (lower).

velocity was controlled at 3.8 mm s^{-1}. We analyzed the mixing and the reaction respectively along the winding channel; the captured images at various units are shown in Fig. 5(b). The probe DNA and PBS solutions were injected into the device to mix. The solution fluids were obviously mixed uniformly at the fifth curved unit by virtue of the converging–diverging design of the curved unit to boost fluid mixing. With regard to the reaction test, at the first curved unit, the excitation excited mostly the probe DNA, displaying a FAM signal, but an extremely faint TAMRA signal from the target DNA occurred around the material interface between the probe DNA and the target DNA. Once the probe DNA and the target DNA were in contact, hybridization (FRET reaction) merely occurred at the material interface. As the plug moved downstream, the FAM signal gradually weakened and the TAMRA signal increased (see 5th curved unit), implying that the reaction was proceeding in the channel; the TAMRA signal attained a uniform distribution in a plug at a downstream channel (see 25th curved unit).

A mixing index to quantify the mixing is defined as $M_i = (STD_x - STD_\infty)/(STD_0 - STD_\infty)$, in which STD_x is the standard deviation of the fluorescent intensity in a plug at curved unit x^{th}; STD_0 is the standard deviation of the fluorescent intensity in a newly generated plug (with unmixed fluids) near the confluence; STD_∞ is the standard deviation of the fluorescent intensity in a plug with fully mixed fluids. To interpret the reaction, we analyzed the variation of the ratio of fluorescent intensities of TAMRA to FAM (I_{TAMRA}/I_{FAM}) along the channel. M_i and this intensity ratio at varied positions are charted in Fig. 6. That the mixing index increased sharply to unity along the channel reveals that mixing of the fluids in a plug, induced by the converging–diverging channel, was efficient. Mixing index 0.9 was achieved about the third unit; the corresponding mixing period was approximately 0.8 s. The increasing intensity ratio along the channel reveals that the hybridization of probe DNA and target DNA was in progress; the ratio approached 1.2, indicating that the hybridization was in equilibrium in the downstream channel. The duration of hybridization of the DNA was estimated to be about 3.3 s, much smaller than minutes or hours for a microfluidic DNA microarray.[45]

Locally enhanced concentration for low-concentration detection

After the complete reaction of the DNA in the curved channel, the plug moved through the straight channel but the reacted DNA within the plug underwent a locally enhanced concentration. An intense FRET signal occurred at the rear of the plug, which represented most of the double stranded (probe-target) DNA accumulating at the rear as shown in Fig. 7(a). Fig. 7(b) shows a profile of FRET intensity, normalized along a central line in the plug. Two maxima located at the front and rear of the plug were induced by the combined effect. The maximum intensity at the rear zone was more than five times the average intensity. The detected signal at the rear zone was hence amplified at least five-fold, attributed to the locally enhanced concentration, and the intensity ratio (I_{TAMRA}/I_{FAM}) of a VOI at the rear zone was more than 2.5, indicating a highly efficient hybridization occurring at the rear. The efficiency of hybridization of the DNA was likely improved because the DNA aggregated in the rear zone to increase the probability of the DNA collision and hybridization.

To comprehend the detection limit of this system for DNA detection, we performed an analysis of the ratio of signal to noise (SNR) (see Fig. 8). For this purpose, a probe DNA solution of fixed concentration 5 μM was employed to undergo reaction in the device with a target DNA solution of varied concentration, specifically 5 μM, 500 nM, 50 nM and 20 nM. The reacted DNA was concentrated in the straight channel and detected at a position 45 mm. The ratio of signal to noise (SNR) is defined as

$$\mathrm{SNR} = \frac{(I_{TAMRA} - I_b)}{(I_{TAMRA(FAM)} - I_b)} \quad (2)$$

in which I_b corresponds to the background intensity; $I_{TAMRA(FAM)}$ is the TAMRA intensity emanated from FAM (probe DNA) (the emission of FAM partially overlapped the passband of the filter used to detect the TAMRA signal). In the case of SNR for a system being approximately unity, one cannot

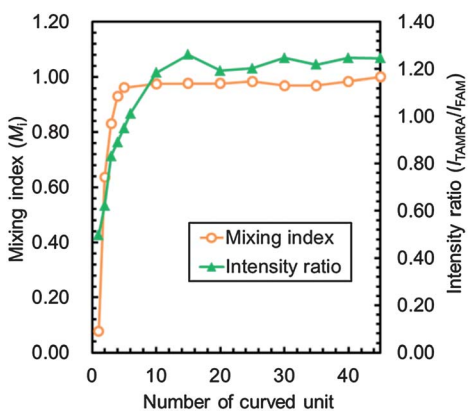

Fig. 6 Variation of mixing index (M_i) and intensity ratio (I_{TAMRA}/I_{FAM}) along the curved units in the winding channel.

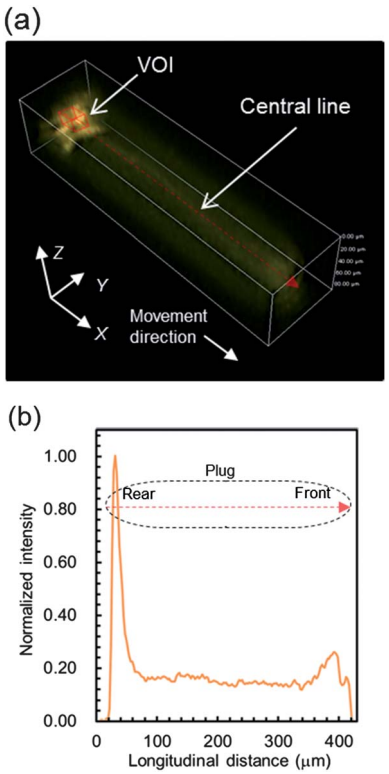

Fig. 7 Concentration results of DNA in a plug at 45 mm of the straight channel after hybridization. (a) 3D distribution of the reacted DNA in a plug after a locally enhanced concentration. (b) Analysis of the intensity profile along a central line in the plug.

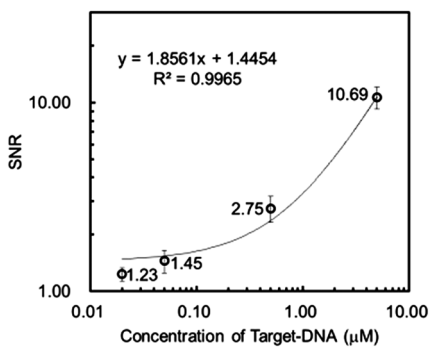

Fig. 8 Analysis of detection limit of the system to detect target DNA.

differentiate the signal from intrinsic fluorescence of TAMRA and the irrelevant signal from fluorescence of FAM in the system.

For a reaction with equimolar (5 μM) probe DNA and target DNA, the detection was achieved at SNR = 10.69. This SNR for the detection decreased with decreasing concentration of target DNA. The best-fitted regression curve exhibits a perfectly linear correlation between the SNR and the concentration of target DNA from 20 nM to 5 μM; R^2 of the curve is 0.9965. If the detection of concentration of target DNA was less than 20 nM, the SNR would be approximately unity and the FRET signal would be negligible relative to the FAM signal. The limit of this system to detect the target was about 20 nM. In previous work a detection limit of target DNA was reported to be 100 nM to 1 μM in a continuous-flow microfluidic device with CFM and a FRET technique.[46] In contrast, as our system took advantage of a locally enhanced concentration in a plug-based microfluidic device, a detection for a small target concentration (20 nM) was accomplished in a plug with a small volume (nL to pL, pL detection is feasible in a smaller microchannel) in seconds.

Conclusions

We discovered that specifically modified DNA within a moving plug is prone to locally enhanced concentration at the rear of the plug in a plug-based microfluidic device. This enhancement of local concentration of DNA was enforced by an entropic force induced by fluid shear (*i.e.* a hydrodynamic-repellent effect) in combination with the effect of affinity occurring at the aqueous/oil interface. Based on a locally enhanced concentration of DNA, a novel technique is proposed to enrich and to detect DNA *in situ* in a free-solution plug with small volume (nL to pL) in seconds.

The formation of the dumbbell-like region with an enhanced concentration of DNA is explained from the perspective of a distribution of the rate of shear strain in flow fields within a plug. Using a confocal fluorescence microscope (CFM) at a large scan rate (230 fps), tests of DNA concentration or enrichment, mixing and reaction (DNA hybridization) executed in devices were monitored; 2D and 3D DNA distributions in a plug were analyzed. In the concentration test, TC-DNA (TAMRA-labeled) displayed a more efficient concentration in a plug than FC-DNA (FAM-labeled) because the concentration of TC-DNA was affected by the combined effect whereas that of FC-DNA was affected by only the hydrodynamic effect; the concentration factor (C_f) of the TC-DNA was twice that of the FC-DNA.

The mixing and reaction tests were conducted in a designed device composed of a winding channel for fluid mixing and reaction, and a straight channel for concentration. The mixing period of a PBS solution and a FC-DNA solution was estimated to be 0.8 s in the device, whereas the hybridization period of probe DNA and target DNA, complementary DNA, was estimated to be 3.3 s by means of the FRET technique (FRET signal occurs as the DNA hybridizes). After hybridization of the probe DNA and the target DNA in the winding channel, the reacted DNA concentrated in the straight channel of length 45 mm. The results show that, at the rear zone of the plug, the FRET intensity was over five times the average intensity, and the intensity ratio (I_{TAMRA}/I_{FAM}) was improved. The hybridization efficiency of the DNA was hence enhanced and the FRET signal was amplified at the rear zone by virtue of the locally enhanced concentration. By examining the ratio of signal to noise (SNR) for detection of varied concentration of the target DNA (with a fixed concentration of the probe DNA), we demonstrated that the detection limit of the proposed technique was 20–50 nM, which is superior to that (100 nM to 1 μM) of the previous technique.[46]

The proposed technique implements the concentration of DNA and the detection of DNA at a small concentration in a nL–pL free-solution plug in seconds in a plug-based device, without additional microfluidic component, medium or external addition, and is hence advantageous to plug-based microfluidics.

This journal is © The Royal Society of Chemistry 2012

Acknowledgements

National Science Council of the Republic of China partially supported this work under contracts NSC 96-2628-E-002-257-MY3, and NSC 99-2221-E-002-103.

References

1 S. Marre and K. F. Jensen, *Chem. Soc. Rev.*, 2010, **39**, 1183–1202.
2 D. T. Chiu, R. M. Lorenz and G. D. M. Jeffries, *Anal. Chem.*, 2009, **81**, 5111–5118.
3 A. B. Theberge, F. Courtois, Y. Schaerli, M. Fishchlechner, C. Abell, F. Hollfelder and W. T. S. Huck, *Angew. Chem., Int. Ed.*, 2010, **49**, 5846–5868.
4 E. Brouzes, M. Medkova, N. Savenelli, D. Marran, M. Twardowski, J. B. Hutchison, J. M. Rothberg, D. R. Link, N. Perrimon and M. L. Samuels, *Proc. Natl. Acad. Sci. U. S. A.*, 2009, **106**, 14195–14200.
5 H. Song and R. F. Ismagilov, *J. Am. Chem. Soc.*, 2003, **125**, 14613–14619.
6 H. Song, D. L. Chen and R. F. Ismagilov, *Angew. Chem., Int. Ed.*, 2006, **45**, 7336–7356.
7 B. Zheng, J. D. Tice, L. S. Roach and R. F. Ismagilov, *Angew. Chem.*, 2004, **116**, 2562–2565.
8 P. S. Dittrich, M. Jahnz and P. Schwille, *ChemBioChem*, 2005, **6**, 811–814.
9 H. Song, H. W. Li, M. S. Munson, T. G. Van Ha and R. F. Ismagilov, *Anal. Chem.*, 2006, **78**, 4839–4849.
10 J. Q. Boedicker, L. Li, T. R. Kline and R. F. Ismagilov, *Lab Chip*, 2008, **8**, 1265–1272.
11 J. Clausell-Tormos, D. Lieber, J. C. Baret, A. El-Harrak, O. J. Miller, L. Frenz, J. Blouwolff, K. J. Humphry, S. Köster, H. Duan, C. Holtze, D. A. Weitz, A. D. Griffiths and C. A. Merten, *Chem. Biol.*, 2008, **15**, 427–437.
12 N. R. Beer, B. J. Hindson, E. K. Wheeler, S. B. Hall, K. A. Rose, I. M. Kennedy and B. W. Colston, *Anal. Chem.*, 2007, **79**, 8471–8475.
13 R. Tewhey, J. B. Warner, M. Nakano, B. Libby, M. Medkova, P. H. David, S. K. Kotsopoulos, M. L. Samuels, J. B. Hutchison, J. W. Larson, E. J. Topol, M. P. Weiner, O. Harismendy, J. Olson, D. R. Link and K. A. Frazer, *Nat. Biotechnol.*, 2009, **27**, 1025–1031.
14 M. Srisa-Art, A. J. deMello and J. B. Edel, *Anal. Chem.*, 2007, **79**, 6682–6689.
15 A. T.-H. Hsieh, P. J.-H. Pan and A. P. Lee, *Microfluid. Nanofluid.*, 2009, **6**, 391–401.
16 N. Pamme, *Lab Chip*, 2007, **7**, 1644–1659.
17 R. Sinville and S. A. Soper, *J. Sep. Sci.*, 2007, **30**, 1714–1728.
18 C. W. Price, D. C. Leslie and J. P. Landers, *Lab Chip*, 2009, **9**, 2484–2494.
19 G. B. Salieb-Beugelaar, K. D. Dorfman, A. van den Berg and J. C. T. Eijkel, *Lab Chip*, 2009, **9**, 2508–2523.
20 B. M. Paegel, C. A. Emrich, G. J. Wedemayer, J. R. Scherer and R. A. Mathies, *Proc. Natl. Acad. Sci. U. S. A.*, 2002, **99**, 574–579.
21 S. H. Kang, M. Park and K. Cho, *Electrophoresis*, 2005, **26**, 3179–3184.
22 M. C. Breadmore, K. A. Wolfe, I. G. Arcibal, W. K. Leung, D. Dickson, B. C. Giordano, M. E. Power, J. P. Ferrance, S. H. Feldman, P. M. Norris and J. P. Landers, *Anal. Chem.*, 2003, **75**, 1880–1886.
23 L. R. Huang, E. C. Cox, R. H. Austin and J. C. Sturm, *Science*, 2004, **34**, 987–990.
24 M. A. Witek, S. D. Llopis, A. Wheatley, R. L. McCarley and S. A. Soper, *Nucleic Acids Res.*, 2006, **34**, e74.
25 J. Fu, R. B. Schoch, A. L. Stevens, S. R. Tannenbaum and J. Han, *Nat. Nanotechnol.*, 2007, **2**, 121–128.
26 L. W. Bezuidenhout, N. Nazemifard, A. B. Jemere, D. J. Harrison and M. J. Brett, *Lab Chip*, 2011, **11**, 1671–1678.
27 J. G. Lee, K. H. Cheong, N. Huh, S. Kim, J. W. Choi and C. Ko, *Lab Chip*, 2006, **6**, 886–895.
28 R. Dhopeshwarkar, L. Sun and R. M. Crooks, *Lab Chip*, 2005, **5**, 1148–1154.
29 R. H. Meltzer, J. R. Krogmeier, L. W. Kwok, R. Allen, B. Crane, J. W. Griffis, L. Knaian, N. Kojanian, G. Malkin, M. K. Nahas, V. Papkov, S. Shaikh, K. Vyavahare, Q. Zhong, Y. Zhou, J. W. Larson and R. Gilmanshin, *Lab Chip*, 2011, **11**, 863–873.
30 J. Y. Yun, S. J. Mun, S. S. Lee and H. G. Nam, *Lab Chip*, 2007, **7**, 916–919.
31 L. S. Roach, H. Song and R. F. Ismagilov, *Anal. Chem.*, 2005, **77**, 785–796.
32 M. N. Kashid, I. Gerlach, S. Goetz, J. Franzke, J. F. Acker, F. Platte, D. W. Agar and S. Turek, *Ind. Eng. Chem. Res.*, 2005, **44**, 5003–5010.
33 M. N. Kashid, F. Platte, D. W. Agar and S. Turek, *J. Comput. Appl. Math.*, 2007, **203**, 487–497.
34 A. Ghaini, A. Mescher and D. W. Agar, *Chem. Eng. Sci.*, 2011, **66**, 1168–1178.
35 W. F. Fang and J. T. Yang, *Sens. Actuators, B*, 2009, **140**, 629–642.
36 S. S. Varghese, Y. Zhu, T. J. Davis and S. C. Trowell, *Lab Chip*, 2010, **10**, 1355–1364.
37 W. F. Fang, M. H. Hsu, Y. T. Chen and J. T. Yang, *Biomicrofluidics*, 2011, **5**, 014111.
38 L. M. Martyushev and V. D. Seleznev, *Phys. Rep.*, 2006, **426**, 1–45.
39 D. E. Smith, H. P. Babcock and S. Chu, *Science*, 1999, **283**, 1724–1727.
40 T. Su and P. K. Purohit, *Phys. Rev. E: Stat., Nonlinear, Soft Matter Phys.*, 2011, **83**, 061906.
41 G. Bao, *J. Mech. Phys. Solids*, 2002, **50**, 2237–2274.
42 C. J. Benham and S. P. Mielke, *Annu. Rev. Biomed. Eng.*, 2005, **7**, 21–53.
43 C. Haber and D. Wirtz, *Biophys. J.*, 2000, **79**, 1530–1536.
44 C. M. Schroeder, R. E. Teixeira, E. S. G. Shaqfeh and S. Chu, *Macromolecules*, 2005, **38**, 1967–1978.
45 L. Wang and P. C. H. Li, *Anal. Chim. Acta*, 2011, **687**, 12–27.
46 L. Chen, S. Lee, M. Lee, C. Lim, J. Choo, J. Y. Park, S. Lee, S. W. Joo, K. H. Lee and Y. W. Choi, *Biosens. Bioelectron.*, 2008, **23**, 1878–1882.